

# Performance of Automatic Active Space Selection for Electronic Excitation Energies

Reza G. Shirazi, Alexander Zech, Peter Pinski, and Vladimir V. Rybkin\*

*HQS Quantum Simulations GmbH, Rintheimer Str. 23, D-76131 Karlsruhe, Germany*

E-mail: vladimir.rybkin@quantumsimulations.de

## Abstract

Computation of electronic spectra is one of the most important applications of methods capturing static electron correlation, including complete-active-space self-consistent field (CASSCF) and post-CASSCF theories. Performance of these techniques critically depends on the active space construction, both in terms of accuracy and computational effort. In this work we benchmark the performance of automatic active space construction, as implemented in the Active Space Finder software, for the computation of electronic excitation energies. The multi-step procedure constructs meaningful molecular orbitals and selects the most suitable active space based on information from more approximate correlated calculations. It aims to tackle a key difficulty in computing excitation energies with CASSCF: choosing active spaces that are balanced for several electronic states. The Active Space Finder is tested with several established data sets of small and medium-sized molecules and shows encouraging results. We evaluate multiple setting configurations and provide practical recommendations.

## Introduction

The complete active-space self-consistent-field (CASSCF) method and multireference approaches based on it are standard tools to capture static (strong) electron correlation.<sup>1</sup> Not always pro-

nounced in the electronic ground states, static correlation is significantly more common in excited states, making multireference approaches an indispensable tool for electronic spectroscopy and photochemistry.<sup>2</sup> A well-known disadvantage of these techniques is the necessity to choose suitable orbitals for the active space. Traditionally, this is done manually, requiring insight into both the CASSCF method and the problem at hand, and introducing an element of subjectivity into such calculations.<sup>3</sup> The active space size affects both accuracy and time-to-solution: in a straightforward implementation, CASSCF complexity scales exponentially with active space size. This puts a stiff limitation on the number of orbitals that can be included in the active space: increasing their number dramatically increases computational cost, not necessarily improving the accuracy of computed results. Thus, a "good" active space should be suitable to treat the problem at hand, but also sufficiently compact to maintain computational feasibility.

Already a non-trivial task for the ground state, active space construction becomes even more challenging when several states (ground and excited) are considered together, which is needed to compute electronic excitations either by state-averaged or state-specific CASSCF. Thus, development of reliable active space selection techniques can be critical to advance the broader application of multi-reference methods.

Up to now, several strategies for automatic active space selection have been developed. Early approaches were based on natural orbital occupation numbers.<sup>4,5</sup> Recent developments along these lines have lead to adaptive basis sets for correlated wave functions (ABC family)<sup>6,7</sup> and the active space selection based on 1st order perturbation theory (ASS1ST)<sup>8,9</sup> scheme. Another philosophy makes use of quantum information measures: examples are autoCAS,<sup>10,11</sup> which employs entropies to analyze orbital entanglement, and the quantum-information-assisted CAS optimization (QICAS)<sup>12</sup> method. Alternative approaches to active space selection exploit projector/fragment-based techniques. Examples are atomic valence active spaces (AVAS),<sup>13–16</sup> automatic partition of orbital spaces based on singular-value decomposition (SPADE),<sup>14,15</sup> and imposed automatic selection and localization of CAS.<sup>16</sup> Yet another family of methods utilizes ranking/scoring of orbitals particularly appealing for high-throughput calculations.<sup>17,18</sup> Finally, machine learning techniques

and data-driven approaches have found their way into active-space finding.<sup>19,20</sup> Of particular interest for the scope of this work are the methods extended to treat excited states: autoCAS, ABC2 and the dipole moment-based scheme.<sup>21</sup>

Due to the importance of CASSCF and multireference methods for electronic spectroscopy,<sup>22</sup> their performance has been extensively studied; in some cases combined with automatic active space selection methods.<sup>6,17,21,23</sup> This has resulted in readily available databases and datasets, including Thiel's set<sup>24</sup> and the more recent QUESTDB database.<sup>25,26</sup> The former encompasses both theoretical vertical and experimental values for excitation energies into several electronically excited states of 28 molecular systems. The latter is more extensive, contains several subsets<sup>27–32</sup> with hundreds of compounds, and is subject to ongoing updates. Importantly, QUESTDB does not depend on experimental data by design, using high-level theory results as reference values.

Benchmarking multireference methods for electronic excitation energies has multiple facets: choosing the most suitable post-CASSCF electronic theory approach to calculate the dynamic correlation energy; benchmarking basis sets or method/basis combinations; and selecting the most suitable formalism: state-averaged<sup>33</sup> or state-specific. Additional challenges arise if one is interested not only in vertical excitations, but in adiabatic ones and in vibronic structure. In this work, we restrict ourselves to benchmarking the automatic active space finding procedure within the state-averaged formalism for vertical electronic excitations. As a post-CASSCF method to calculate the dynamic part of the correlation energy we chose second-order  $n$ -electron valence state perturbation theory, NEVPT2.<sup>34</sup> We utilize the strongly-contracted scheme for NEVPT2 (SC-NEVPT2),<sup>35</sup> which has been shown to systematically deliver fairly reliable vertical transition energies,<sup>36</sup> only marginally inferior to the partially contracted scheme.<sup>37</sup> While not exhaustive in scope, this approach provides a systematic and unambiguous test for active space construction for several electronic states.

# Methods

## Requirements for automatic active space determination

We believe it is desirable that a generally applicable, user-friendly and computationally affordable technique to find active spaces satisfies the following criteria:

1. it generates orbitals that serve as a good guess for CASSCF, leading to convergence within a reasonable number of iterations;
2. the active space is constructed through an automatic procedure that minimizes the need for manual user intervention and maximizes reproducibility;
3. autonomy: in line with the *ab initio* character of multi-reference methods, the choice is made independently of problem-specific reference data (even though the active space selection procedure may involve parameters of a generic nature);
4. *a priori* character: the choice is made prior to the CASSCF calculation.

At first sight, the final point might appear as a tautology. However, active spaces can be refined by repeating CASSCF calculations with different numbers of active orbitals, especially, if the molecular orbitals from one calculation are taken as a guess for the next one. This approach is not only employed in manual active space selection, but is also used by some automatic schemes.<sup>8,21</sup> The philosophy underlying this work is that the active space should be determined prior to any CASSCF or post-CASSCF calculations, even if they are inexpensive as in ref.<sup>38</sup> This permits the approach to be applied in a more general context to large active spaces, for which calculations may be expensive. It also makes the scheme suitable for methods that do not optimize orbitals, such as complete active space configuration interaction (CASCI).

## Algorithm

This work employs the Active Space Finder (ASF) package,<sup>39</sup> which is published together with its documentation under an open source license. Modifications of the software were made for an improved treatment of excited states as part of this work. Those changes will be released in the publically available software repository in due course. A detailed description of the principles underlying the ASF software, with a focus on ground states, is in preparation for a forthcoming manuscript. Therefore, the algorithm is explained below only in general terms, and a description of the modifications made for excited states is provided.

The central component of our active space finding procedure is a density matrix renormalization group (DMRG)<sup>40</sup> calculation performed with low-accuracy settings. This idea is related to the autoCAS method by Reiher and co-workers.<sup>10</sup> However, the analysis of the DMRG results to determine an active space employs profoundly different principles. Prior to performing the DMRG calculation, an initial active space needs to be selected. It has to be sufficiently large, such that it contains all orbitals that will be part of the final active space. At the same time, it must be sufficiently small to keep the effort for the DMRG calculation feasible. The individual steps are described in more detail below.

**Self-consistent field calculation** as the first step. The fully automatic mode of the ASF always employs the spin-unrestricted Hartree-Fock (UHF) method. A stability analysis is performed with the converged orbitals, followed by a restart of the calculation if there is an internal instability. Pulay and co-workers demonstrated the utility of unrestricted natural orbitals (UNOs) for the selection of minimal active spaces.<sup>4,41</sup> We do not calculate UNOs, but we employ symmetry breaking in a similar spirit. Therefore, UHF calculations are initiated even if the system has singlet multiplicity. However, it is also possible to carry out a restricted Hartree-Fock (RHF) calculation manually and to use it to proceed further with the ASF software.

**Selection of an initial space.** Even relatively small molecules may possess hundreds of occupied

and virtual molecular orbitals with a basis set suited for correlated calculations. An initial active space, which may be substantially larger than the final space, needs to be determined in order to keep the computational effort manageable for the subsequent steps. All procedures used in the present work employ natural orbitals of an orbital-unrelaxed second-order Møller-Plesset perturbation theory (MP2) density matrix for the ground state. With the help of an occupation number threshold, an initial set of orbitals is selected, and further orbitals are discarded if their number exceeds an upper limit. It is important to omit orbital relaxation effects, as these lead to artifacts with unphysical eigenvalues of the density matrix below zero or above two. A density-fitting MP2 implementation is used for the sake of efficiency. It is particularly beneficial to employ the UHF solution from the first step as a reference wave function for the MP2 calculation. We tested two different ways to represent the initial active space:

1. In the first variant, the MP2 natural orbitals are propagated to the next step. Therefore, the finally chosen active space will be a subset of the MP2 natural orbitals selected for the initial active space.
2. Ground state MP2 natural orbitals are not necessarily the most appropriate orbital set for excited electronic states. Therefore, we implemented a re-canonicalization of the initial space in a procedure that is analogous to quasi-restricted orbitals (QROs).<sup>42</sup> In contrast to the QRO procedure, the respective Fock matrix sub-blocks are projected to the initial active space constructed from MP2 natural orbitals prior to diagonalization. This ensures that the initial space is preserved without mixing in other orbitals, even though it is represented by orbitals resembling a restricted open-shell Hartree-Fock (ROHF) solution. In contrast to using ROHF orbitals or QROs directly, our procedure provides a clear-cut selection of a sufficiently, but manageably large initial active space through the occupation number threshold for MP2 natural orbitals.

**Approximate CASCI calculation** to determine correlation information for the final active space

selection. This step is carried out as a DMRG-CASCI calculation with a low matrix product state bond dimension. If the size of the initial space is sufficiently small (typically up to 14 orbitals), a regular CASCI calculation can be performed instead. It is important to point out that the nature of the initial space selection determines the type of molecular orbitals used in the (DMRG-)CASCI calculation and for the final active space selection. Thus the molecular orbitals used throughout the calculation will be MP2 natural orbitals, QROs, or another basis, depending on the initial choice.

**Analysis of the correlation information** from the (DMRG-)CASCI calculation. An important design goal of the ASF was to identify correlation partner orbitals. This is accomplished through an automatic analysis of the two-electron cumulant. It has previously been discussed in the literature as a measure for electron correlation,<sup>43,44</sup> but the ASF is, to the best of our knowledge, the first method employing it for active space selection. In contrast to mutual information calculated from two-orbital entropies,<sup>10</sup> which include contributions of reduced density matrix elements of up to fourth order,<sup>45</sup> only the two-electron density matrix is required to compute the two-electron cumulant.

Analysis of the cumulant leads to multiple suggestions for sensible active spaces of different sizes. In order to select one of these active spaces, the one-orbital entropy is used as an auxiliary criterion.<sup>45,46</sup> An entropy threshold is defined as a target value. For all active space suggestions identified through analysis of the cumulant, the lowest entropy of all orbitals in the active space is compared to the target value. The active space with its lowest entropy closest to the target value is selected as the final choice.

Extensions of the aforementioned algorithm were made in order to construct active spaces suitable for the treatment of excited states with state-averaged CASSCF. We implemented two strategies:

**Union of individual active spaces.** The (DMRG-)CASCI density matrices are calculated for all relevant electronic states. Subsequently, the correlation information for each electronic state

is analyzed to determine one space per electronic state independently. Finally, a combined active space is created as the union: every orbital that is member of an active space of at least one electronic state becomes a member of the combined space.

**Averaging of electronic states.** Instead of forming the union of multiple active spaces determined for each state individually, active spaces are determined for multiple states at once. For this purpose, averages of the cumulant of the one-orbital density are formed. We define the two-electron cumulant  ${}_n^2\lambda_{rs}^{pq}$  for a single electronic state  $n$  in terms of the respective reduced density matrices:

$${}_n^2\lambda_{rs}^{pq} = \langle \Psi_n | \hat{a}_p^\dagger \hat{a}_q^\dagger \hat{a}_s \hat{a}_r | \Psi_n \rangle - \langle \Psi_n | \hat{a}_p^\dagger \hat{a}_r | \Psi_n \rangle \langle \Psi_n | \hat{a}_q^\dagger \hat{a}_s | \Psi_n \rangle + \langle \Psi_n | \hat{a}_p^\dagger \hat{a}_s | \Psi_n \rangle \langle \Psi_n | \hat{a}_q^\dagger \hat{a}_r | \Psi_n \rangle. \quad (1)$$

Here,  $p, q, r, s$  refer to spin orbitals, while  $\Psi_n$  represent the CASCI wave functions of the respective electronic state. An averaged cumulant is constructed for multiple electronic states  $N_{\text{states}}$ , assuming equal weighting:

$${}^2\bar{\lambda}_{rs}^{pq} = N_{\text{states}}^{-1} \sum_n {}_n^2\lambda_{rs}^{pq} \quad (2)$$

Instead of analyzing the cumulant of each state individually, the algorithm is applied directly to  ${}^2\bar{\lambda}_{rs}^{pq}$ . Multiple suggestions for active spaces of different sizes are determined for state-averaged calculations analogously as for ground states.

In order to select a single space, entropies are determined from an averaged one-orbital density:

$$s_i = - \sum_{\alpha}^{-,\uparrow,\downarrow,\uparrow\downarrow} \bar{\omega}_{i,\alpha} \ln \bar{\omega}_{i,\alpha} \quad (3)$$

The averaged one-orbital density  $\bar{\omega}_{i,\alpha}$  for each spatial orbital  $i$  is calculated using the respec-

tive one-orbital density  $\omega_{i,\alpha}^n$  of each state  $n$ :

$$\bar{\omega}_{i,\alpha} = N_{\text{states}}^{-1} \sum_n^{N_{\text{states}}} \omega_{i,\alpha}^n \quad (4)$$

The same set of orbitals must be used for each electronic state; this is particularly important to recognize if the active space is chosen for more than one spin state. Often, it will be advantageous to perform the Hartree-Fock calculation, and the subsequent MP2 calculation (if applicable), for the state with the highest spin multiplicity. That single set of orbitals can be used for DMRG-CASCI calculations for different spin states to determine the final active space.

For technical reasons, active space selection via averaging of the cumulant and of the one-orbital density have been implemented for electronic states of the same multiplicity only. When determining an active space for state-averaged CASSCF calculations with more than one spin state, it is still possible to employ the averaging procedure for each multiplicity separately; however, the final active space is obtained as the union of the spaces determined with averaging for each respective spin-state only. In principle, it would be conceivable to extend the procedure such that it averages the relevant quantities over multiple spin states using appropriate weighting factors.

## Details of the ASF Calculation

Several calculation variants were tested by altering the following parameters:

- Entropy Threshold: the default value for the entropy threshold in the ASF is set to  $0.1 * \log(4) \approx 0.14$ . We also tested the selection of larger active spaces obtained with a somewhat lower entropy threshold of 0.11. Calculations utilizing the low entropy threshold are denoted as “l-ASF”, whereas “ASF” stands for the default threshold.
- Spin in the HF (SCF) calculation: in some scenarios, it is beneficial to generate guess orbitals for excited states through an SCF calculation with triplet spin multiplicity. As a result, MP2 natural orbitals are also calculated for the lowest triplet state using the UHF solution as the

reference. After truncation to an initial active space, (DMRG-)CASCI calculations and the subsequent active space selection steps are performed for the respective singlet states; only the molecular orbital coefficients originate from a triplet state calculation. Such calculations, employing triplet state guess orbitals, are denoted with “ASF(T)”. Calculations performed with singlet spin multiplicity throughout are indicated by “ASF(S)”.

- Rotation of triplet-state orbitals: UHF-MP2 natural orbitals are often an excellent guess for ground-state CASSCF calculations. However, for excited states it is often preferable to employ orbitals with shapes holding closer semblance to a canonical Hartree-Fock solution. For this reason, the ASF provides functionality to transform the initial active space to a QRO-like solution, without mixing between the initial active and inactive spaces. We performed calculations where the orbitals were obtained using UHF and MP2 calculations for the triplet state, as in ASF(T), but subsequently rotated with the QRO transformation. These calculations are referred with QRO in parentheses: “ASF(QRO)”.
- Calculations reported in this work determined active spaces by averaging cumulants and one-orbital densities over the lowest two singlet states, and analyzing the averaged quantities. Reporting results with unions of active spaces determined individually for each state will be left to future work.
- In order to avoid accidental convergence to higher states, the (DMRG-)CASCI calculations for active space selection were performed for the lowest four electronic states. However, active spaces were determined only for the lowest two singlet states, with the cumulant and the one-orbital density averaged only over these two states.

The various simulation options are summarized in Table 1.

## Computational set-up

This work employs the *Active Space Finder (ASF)* package,<sup>39</sup> which is developed in Python, and built on top of the *PySCF*<sup>47</sup> and *Block2*<sup>48</sup> packages. The code changes for excited states, which are

Table 1: Acronyms for active-space-finding schemes with basic properties.

Entropy threshold = 0.14	ASF(S)	ASF(T)	ASF(QRO)
Entropy threshold = 0.11	I-ASF(S)	I-ASF(T)	I-ASF(QRO)
Spin in SCF	S = 1	S = 3	S = 3
Initial orbitals	MP2(S = 1)	MP2(S = 3)	MP2(S = 3)
Rotation on initial active space	natural	natural	QRO
Spin in ASF	S=1	S=1	S=1

subject to testing in this work, were implemented in a development version of the ASF that will be made available publically in due course. PySCF was used for all quantum chemistry calculations, including CASSCF<sup>49</sup> and SC-NEVPT2.<sup>37</sup> Block2<sup>50</sup> was employed via its PySCF interface for DMRG calculations called by the ASF.

The triple-zeta quality basis set with diffuse functions def2-TZVPD<sup>51,52</sup> was used for all calculations. Resolution-of-identity (or density fitting)<sup>53</sup> was applied to accelerate electron repulsion integral evaluation using the corresponding auxiliary basis sets.<sup>54</sup> Excitation energies were computed using state-averaged CASSCF with equal weights for the ground and the first excited state. Dynamic correlation energy contributions were calculated using the strongly contracted NEVPT2 formalism.

This work focuses on vertical excitation energies between the ground and the first excited state, which were computed using accurate ground state equilibrium geometries taken from literature.

## Testing data sets

Testing was performed with 32 small and medium-sized molecules from Thiel's data set<sup>24</sup> and from the paper of Hoyer *et al.*<sup>23</sup> This work employs molecular geometries and reference excitation energies as described in those articles. For molecules that are present in both papers, we chose the data from the more recent work in ref. 23. The complete list of molecules is available in the SI.

## Results and Discussion

The results of calculations using ASF are summarized in Table 2 and Figure 1, whereas the full data are given in the SI. Active space selection is not a problem with a uniquely defined solution: depending on the problem at hand and the electronic structure method employed, active spaces of different size may be suitable for the same molecule. This work takes a pragmatic approach: it examines how well automatic active space selection and correlated calculations work together in reproducing reference excitation energies.

We assign calculation results into three categories: failure (CASSCF has not reached convergence), miss (mean absolute deviation, MAE, from the reference value is larger than 1 eV) and satisfactory performance. If CASSCF fails to converge, which is typically a clear sign of improper active-space selection, the deviation is assigned the value of the reference excitation energy.

Table 2: Main benchmarking results: "fail" represents the number of systems with CASSCF convergence failure; "miss" denotes the number of systems with absolute deviation from the reference larger than 1 eV; MAE is the mean average error with respect to reference values for the entire data set of 32 molecules.

method	l-ASF(QRO)	l-ASF(S)	l-ASF(T)	ASF(QRO)	ASF(S)	ASF(T)	combined
fail	0	3	2	1	2	2	1
miss	7	3	5	8	8	8	3
MAE	0.49	0.75	0.87	0.67	0.83	0.85	0.51

First, we note that for any of the tested schemes number of failures does not exceed 3 out of 32, whereas the maximum number of misses and failures is 10, just below one third. MAE for the entire dataset is below 1 eV for all schemes. For both values of entropy thresholds, rotating the initially selected MP2 natural orbitals with the QRO transformation leads to improved performance. The best results are obtained with the “l-ASF(QRO)” scheme, which combines triplet state guess orbitals with a QRO transformation and a lowered entropy threshold: with these active spaces, all CASSCF calculations converged giving only eight misses, whereas MAE is slightly above 0.5 eV.

It is useful to understand the reasons behind failures and misses to be able to propose a diagnostic for the sanity of results without comparing to the reference. One cause of unsatisfactory

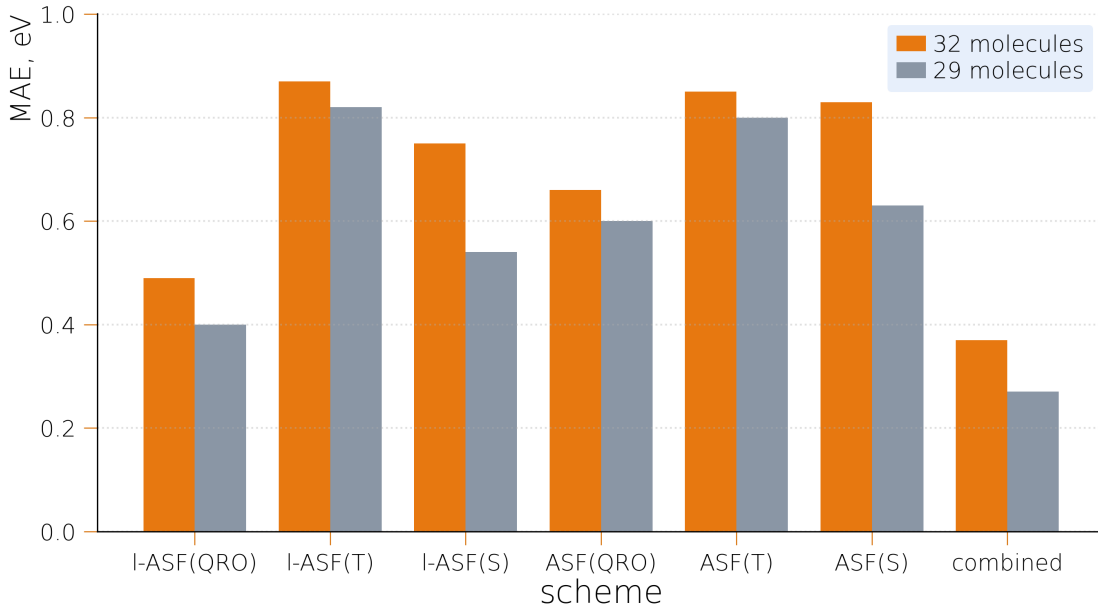


Figure 1: Mean absolute errors wrt. benchmark excitation energies values for the test data set. Blue - the entire data set of 32 molecules; orange - reduced data set (29 molecules).

performance is the presence of a near-degenerate excited state not considered by state averaging. This can lead to root-swapping in the CASSCF procedure. Additionally, some perturbation theories for dynamic correlation are prone to intruder states. Para-benzoquinone is a notorious example: its first and second singlet excited states are separated by ca. 0.2 eV according to the experiments (and less than 0.1 eV depending on the theory level).<sup>24</sup> Therefore, our set-up considering ground and first excited state only leads to either miss or failure in all applied schemes. One can remedy this problem by inspecting excited states at Step 3 of the algorithm: fast DMRG calculation can include more excited states than needed in the production run to estimate the possibility of near-degeneracy. Although DMABN molecule does not have such near-degenerate levels, averaging over more states is known to increase the accuracy of multireference calculations of its electronic spectra critically.<sup>55</sup>

An additional reason for unsatisfactory performance is that larger active spaces are needed than those determined by the ASF with default settings. For propanamide, all protocols result find an (4,4) active space, result in failures and misses. Analysis of the active orbitals shows that the

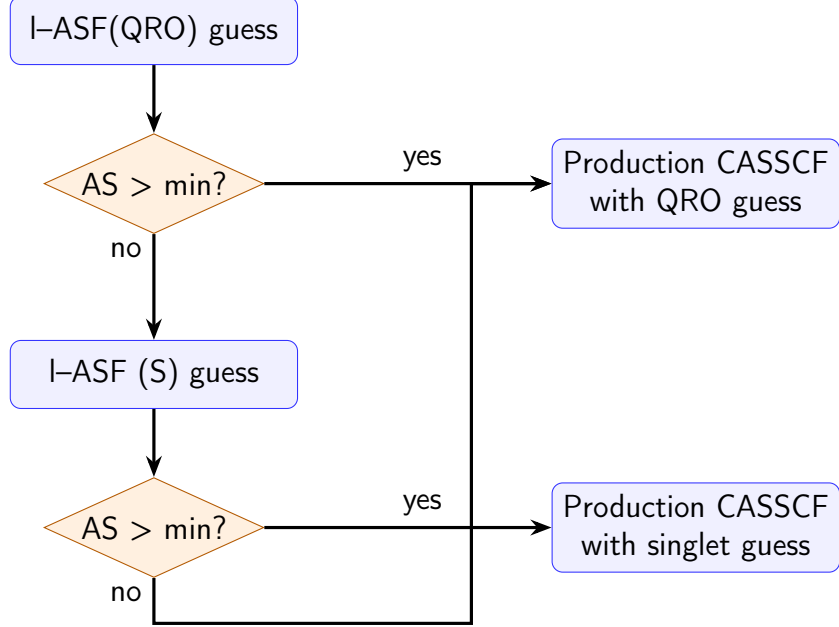


Figure 2: A combined ASF protocol: one loops over guess orbitals generation methods until the active space has more than three virtual orbitals, which is denoted as *min* in the diagram. The order of the methods is: 1) QRO, 2) singlet (S) based on their performance. In rare case where both methods suggest a small active space, a QRO guess should be used.

calculations converge to an electronic state different from the true first excited  $n \rightarrow \pi^*$  one. This is a sign that more states must be considered for state averaging. In the case of cyclopentadiene, the only protocol delivering accurate results (error of just 0.13 eV) is l-ASF(S), which determines an (8,8) active space, whereas other schemes suggest (4,4) active spaces and perform unsatisfactorily. For formamide, not only a (4,4) but also a (6,6) active space lead to significant errors; only ASF(S) and l-ASF(S) lead to accurate values, as they determine larger (8,9) active spaces. Therefore, we recommend to avoid production calculations if a small active space is generated by the selected scheme. Instead, active-space construction should be reconsidered with either the orbital entropy threshold relaxed, or with a different choice of initial orbitals.

Inspired by these results, we have designed a combined protocol shown in Figure 2, which addresses the issue of small active spaces. The first step is an l-ASF(QRO) calculation. If the active space thereby generated contains fewer than three unoccupied orbitals, l-ASF(S) is used, instead. If this scheme results in a small active space, too, one should perform a production CASSCF calculation with an active space from l-ASF(QRO). The only and notorious exception is the water

molecule, for which a small (4,5) active space is balanced and provided very accurate excitation energies, whereas a larger (6,6) active space from l-ASF(S) leads to larger errors. Despite its importance, water is a small system and it is not representative.

To get a clearer picture, we have considered a reduced data set by removing molecules requiring averaging over more than two states: propanamide, benzoquinone and DMABN. The performance of all protocols is considerably improved, especially for the combined scheme 1. Independently of this, we have been able to achieve accurate results for p-benzoquinone and propanamide by averaging over four electronic states. However, consideration of multiple electronic excitations goes beyond the scope of the current work.

## Conclusions

We have designed and tested automatic active space selection protocols to compute excitation energies with multi-reference methods. To this end, we worked with the publically available “Active Space Finder” (ASF)<sup>39</sup> software. Employing multiple levels of correlated calculations, it constructs suitable orbitals and selects active spaces with the help of the two-electron cumulant and one-orbital entropies. As part of this work, the implementation was adapted for an improved treatment of excited states targeting state-averaged CASSCF.

Testing its performance for electronic excitation energies of a set of small and medium-sized organic molecules reveals reasonable performance: with all schemes employed the percentage of unsatisfactory results varies from 25 to 30% in fully automatic mode. The best-performing scheme utilizes a slightly lowered entropy threshold for active orbital selection and is based on quasi-restricted orbitals (QRO) transformed within an initial space constructed from MP2 natural orbitals.

Error analysis has revealed two main sources of poor performance: the presence of quasi-degenerate excited states not considered in the calculation and small sizes of active spaces. Both can be remedied by averaging over more excited states, repeating the preliminary calculations with

a different orbital entropy criterion and/or alternative choice of initial orbitals. Such modifications are easy to customize and can be readily streamlined for high-throughput calculations. We have proposed a simple combined workflow addressing the problem of small active sizes, which significantly reduces the errors.

## Acknowledgements

This work has received funding from the German Federal Ministry of Research, Technology and Space (BMFTR) within the PhoQuant project (Grant No. 13N16103) and the PASQUOPS project (Grant No. 13N17251). The Active Space Finder software was developed in collaboration with and with support by Covestro Deutschland AG.

## References

- (1) Roos, B. O. The complete active space self-consistent field method and its applications in electronic structure calculations. *Advances in Chemical Physics: Ab Initio Methods in Quantum Chemistry Part 2* **1987**, *69*, 399–445.
- (2) Lischka, H.; Nachtigallová, D.; Aquino, A. J. A.; Szalay, P. G.; Plasser, F.; Machado, F. B. C.; Barbatti, M. Multireference Approaches for Excited States of Molecules. *Chemical Reviews* **2018**, *118*, 7293–7361, PMID: 30040389.
- (3) Veryazov, V.; Malmqvist, P. Å.; Roos, B. O. How to select active space for multiconfigurational quantum chemistry? *International Journal of Quantum Chemistry* **2011**, *111*, 3329–3338.
- (4) Pulay, P.; Hamilton, T. P. UHF natural orbitals for defining and starting MC-SCF calculations. *The Journal of chemical physics* **1988**, *88*, 4926–4933.

(5) Jensen, H. J. A.; Jørgensen, P.; Ågren, H.; Olsen, J. Second-order Møller–Plesset perturbation theory as a configuration and orbital generator in multiconfiguration self-consistent field calculations. *The Journal of chemical physics* **1988**, *88*, 3834–3839.

(6) Bao, J. J.; Dong, S. S.; Gagliardi, L.; Truhlar, D. G. Automatic Selection of an Active Space for Calculating Electronic Excitation Spectra by MS-CASPT2 or MC-PDFT. *Journal of Chemical Theory and Computation* **2018**, *14*, 2017–2025, PMID: 29486125.

(7) Bao, J. J.; Truhlar, D. G. Automatic Active Space Selection for Calculating Electronic Excitation Energies Based on High-Spin Unrestricted Hartree–Fock Orbitals. *Journal of Chemical Theory and Computation* **2019**, *15*, 5308–5318, PMID: 31411880.

(8) Khedkar, A.; Roemelt, M. Active Space Selection Based on Natural Orbital Occupation Numbers from n-Electron Valence Perturbation Theory. *Journal of Chemical Theory and Computation* **2019**, *15*, 3522–3536, PMID: 31059643.

(9) Khedkar, A.; Roemelt, M. Extending the ASS1ST Active Space Selection Scheme to Large Molecules and Excited States. *Journal of Chemical Theory and Computation* **2020**, *16*, 4993–5005, PMID: 32644789.

(10) Stein, C. J.; Reiher, M. Automated Selection of Active Orbital Spaces. *Journal of Chemical Theory and Computation* **2016**, *12*, 1760–1771, PMID: 26959891.

(11) Stein, C. J.; Reiher, M. autoCAS: A program for fully automated multiconfigurational calculations. *Journal of computational chemistry* **2019**, *40*, 2216–2226.

(12) Ding, L.; Knecht, S.; Schilling, C. Quantum Information-Assisted Complete Active Space Optimization (QICAS). *The Journal of Physical Chemistry Letters* **2023**, *14*, 11022–11029, PMID: 38047727.

(13) Sayfutyarova, E. R.; Sun, Q.; Chan, G. K.-L.; Knizia, G. Automated Construction of Molec-

ular Active Spaces from Atomic Valence Orbitals. *Journal of Chemical Theory and Computation* **2017**, *13*, 4063–4078, PMID: 28731706.

(14) Claudino, D.; Mayhall, N. J. Automatic Partition of Orbital Spaces Based on Singular Value Decomposition in the Context of Embedding Theories. *Journal of Chemical Theory and Computation* **2019**, *15*, 1053–1064.

(15) Kolodzeiski, E.; Stein, C. J. Automated, Consistent, and Even-Handed Selection of Active Orbital Spaces for Quantum Embedding. *Journal of Chemical Theory and Computation* **2023**, *19*, 6643–6655, PMID: 37775093.

(16) Lei, Y.; Suo, B.; Liu, W. iCAS: Imposed Automatic Selection and Localization of Complete Active Spaces. *Journal of Chemical Theory and Computation* **2021**, *17*, 4846–4859, PMID: 34314180.

(17) King, D. S.; Gagliardi, L. A Ranked-Orbital Approach to Select Active Spaces for High-Throughput Multireference Computation. *Journal of Chemical Theory and Computation* **2021**, *17*, 2817–2831, PMID: 33860669.

(18) King, D. S.; Hermes, M. R.; Truhlar, D. G.; Gagliardi, L. Large-Scale Benchmarking of Multireference Vertical-Excitation Calculations via Automated Active-Space Selection. *Journal of Chemical Theory and Computation* **2022**, *18*, 6065–6076, PMID: 36112354.

(19) Jeong, W.; Stoneburner, S. J.; King, D.; Li, R.; Walker, A.; Lindh, R.; Gagliardi, L. Automation of Active Space Selection for Multireference Methods via Machine Learning on Chemical Bond Dissociation. *Journal of Chemical Theory and Computation* **2020**, *16*, 2389–2399, PMID: 32119542.

(20) Golub, P.; Antalik, A.; Veis, L.; Brabec, J. Machine Learning-Assisted Selection of Active Spaces for Strongly Correlated Transition Metal Systems. *Journal of Chemical Theory and Computation* **2021**, *17*, 6053–6072, PMID: 34570505.

(21) Kaufold, B. W.; Chintala, N.; Pandeya, P.; Dong, S. S. Automated Active Space Selection with Dipole Moments. *Journal of Chemical Theory and Computation* **2023**, *19*, 2469–2483, PMID: 37040135.

(22) Helmich-Paris, B. Benchmarks for Electronically Excited States with CASSCF Methods. *Journal of Chemical Theory and Computation* **2019**, *15*, 4170–4179, PMID: 31136706.

(23) Hoyer, C. E.; Ghosh, S.; Truhlar, D. G.; Gagliardi, L. Multiconfiguration Pair-Density Functional Theory Is as Accurate as CASPT2 for Electronic Excitation. *The Journal of Physical Chemistry Letters* **2016**, *7*, 586–591, PMID: 26794241.

(24) Schreiber, M.; Silva-Junior, M. R.; Sauer, S.; Thiel, W. Benchmarks for electronically excited states: CASPT2, CC2, CCSD, and CC3. *The Journal of chemical physics* **2008**, *128*.

(25) Véril, M.; Scemama, A.; Caffarel, M.; Lipparini, F.; Boggio-Pasqua, M.; Jacquemin, D.; Loos, P.-F. QUESTDB: A database of highly accurate excitation energies for the electronic structure community. *WIREs Computational Molecular Science* **2021**, *11*, e1517.

(26) Loos, P.-F.; Boggio-Pasqua, M.; Blondel, A.; Lipparini, F.; Jacquemin, D. QUEST Database of Highly-Accurate Excitation Energies. *Journal of Chemical Theory and Computation* **0**, *0*, null, PMID: 40778852.

(27) Loos, P.-F.; Scemama, A.; Blondel, A.; Garniron, Y.; Caffarel, M.; Jacquemin, D. A Mountaineering Strategy to Excited States: Highly Accurate Reference Energies and Benchmarks. *Journal of Chemical Theory and Computation* **2018**, *14*, 4360–4379, PMID: 29966098.

(28) Loos, P.-F.; Boggio-Pasqua, M.; Scemama, A.; Caffarel, M.; Jacquemin, D. Reference Energies for Double Excitations. *Journal of Chemical Theory and Computation* **2019**, *15*, 1939–1956.

(29) Loos, P.-F.; Lipparini, F.; Boggio-Pasqua, M.; Scemama, A.; Jacquemin, D. A Mountaineering Strategy to Excited States: Highly Accurate Energies and Benchmarks for Medium Sized

Molecules. *Journal of Chemical Theory and Computation* **2020**, *16*, 1711–1741, PMID: 31986042.

- (30) Loos, P.-F.; Scemama, A.; Boggio-Pasqua, M.; Jacquemin, D. Mountaineering Strategy to Excited States: Highly Accurate Energies and Benchmarks for Exotic Molecules and Radicals. *Journal of Chemical Theory and Computation* **2020**, *16*, 3720–3736, PMID: 32379442.
- (31) Loos, P.-F.; Comin, M.; Blase, X.; Jacquemin, D. Reference Energies for Intramolecular Charge-Transfer Excitations. *Journal of Chemical Theory and Computation* **2021**, *17*, 3666–3686, PMID: 33955742.
- (32) Loos, P.-F.; Jacquemin, D. A Mountaineering Strategy to Excited States: Highly Accurate Energies and Benchmarks for Bicyclic Systems. *The Journal of Physical Chemistry A* **2021**, *125*, 10174–10188, PMID: 34792354.
- (33) Werner, H.; Meyer, W. A quadratically convergent MCSCF method for the simultaneous optimization of several states. *The Journal of Chemical Physics* **1981**, *74*, 5794–5801.
- (34) Angeli, C.; Cimiraglia, R.; Evangelisti, S.; Leininger, T.; Malrieu, J.-P. Introduction of n-electron valence states for multireference perturbation theory. *The Journal of Chemical Physics* **2001**, *114*, 10252–10264.
- (35) Angeli, C.; Cimiraglia, R.; Malrieu, J.-P. N-electron valence state perturbation theory: a fast implementation of the strongly contracted variant. *Chemical Physics Letters* **2001**, *350*, 297–305.
- (36) Sarkar, R.; Loos, P.-F.; Boggio-Pasqua, M.; Jacquemin, D. Assessing the Performances of CASPT2 and NEVPT2 for Vertical Excitation Energies. *Journal of Chemical Theory and Computation* **2022**, *18*, 2418–2436, PMID: 35333060.
- (37) Angeli, C.; Cimiraglia, R.; Malrieu, J.-P. n-electron valence state perturbation theory: A

spinless formulation and an efficient implementation of the strongly contracted and of the partially contracted variants. *The Journal of Chemical Physics* **2002**, *117*, 9138–9153.

(38) Shirazi, R. G.; Rybkin, V. V.; Marthaler, M.; Golubev, D. S. Efficient random phase approximation for diradicals. *The Journal of Chemical Physics* **2024**, *161*, 114110.

(39) Active Space Finder. GitHub repository. [Online]. Available: <https://github.com/HQSquantumsimulations/ActiveSpaceFinder>, 2025; Accessed: Oct. 2, 2025.

(40) Chan, G. K.-L.; Sharma, S. The density matrix renormalization group in quantum chemistry. *Annual review of physical chemistry* **2011**, *62*, 465–481.

(41) Keller, S.; Boguslawski, K.; Janowski, T.; Reiher, M.; Pulay, P. Selection of active spaces for multiconfigurational wavefunctions. *The Journal of Chemical Physics* **2015**, *142*, 244104.

(42) Neese, F. Importance of Direct Spin-Spin Coupling and Spin-Flip Excitations for the Zero-Field Splittings of Transition Metal Complexes: A Case Study. *Journal of the American Chemical Society* **2006**, *128*, 10213–10222, PMID: 16881651.

(43) Kong, L.; Valeev, E. F. A novel interpretation of reduced density matrix and cumulant for electronic structure theories. *The Journal of Chemical Physics* **2011**, *134*.

(44) Hanauer, M.; Köhn, A. Meaning and magnitude of the reduced density matrix cumulants. *Chemical Physics* **2012**, *401*, 50–61.

(45) Boguslawski, K.; Tecmer, P. Orbital entanglement in quantum chemistry. *International Journal of Quantum Chemistry* **2015**, *115*, 1289–1295.

(46) Boguslawski, K.; Tecmer, P.; Legeza, Ö.; Reiher, M. Entanglement Measures for Single- and Multireference Correlation Effects. *The Journal of Physical Chemistry Letters* **2012**, *3*, 3129–3135, PMID: 26296018.

(47) Sun, Q.; Berkelbach, T. C.; Blunt, N. S.; Booth, G. H.; Guo, S.; Li, Z.; Liu, J.; McClain, J. D.; Sayfutyarova, E. R.; Sharma, S.; Wouters, S.; Chan, G. K.-L. PySCF: the Python-based simulations of chemistry framework. *WIREs Computational Molecular Science* **2018**, *8*, e1340.

(48) Zhai, H.; Larsson, H. R.; Lee, S.; Cui, Z.-H.; Zhu, T.; Sun, C.; Peng, L.; Peng, R.; Liao, K.; Tölle, J.; Yang, J.; Li, S.; Chan, G. K.-L. Block2: A comprehensive open source framework to develop and apply state-of-the-art DMRG algorithms in electronic structure and beyond. *The Journal of Chemical Physics* **2023**, *159*, 234801.

(49) Sun, Q.; Yang, J.; Chan, G. K.-L. A general second order complete active space self-consistent-field solver for large-scale systems. *Chemical Physics Letters* **2017**, *683*, 291–299, Ahmed Zewail (1946-2016) Commemoration Issue of Chemical Physics Letters.

(50) Zhai, H.; Chan, G. K.-L. Low communication high performance ab initio density matrix renormalization group algorithms. *The Journal of Chemical Physics* **2021**, *154*, 224116.

(51) Weigend, F.; Ahlrichs, R. Balanced basis sets of split valence, triple zeta valence and quadruple zeta valence quality for H to Rn: Design and assessment of accuracy. *Phys. Chem. Chem. Phys.* **2005**, *7*, 3297–3305.

(52) Rappoport, D.; Furche, F. Property-optimized Gaussian basis sets for molecular response calculations. *The Journal of Chemical Physics* **2010**, *133*, 134105.

(53) Vahtras, O.; Almlöf, J.; Feyereisen, M. Integral approximations for LCAO-SCF calculations. *Chemical Physics Letters* **1993**, *213*, 514–518.

(54) Weigend, F. Hartree–Fock exchange fitting basis sets for H to Rn. *Journal of Computational Chemistry* **2008**, *29*, 167–175.

(55) Galván, I. F.; Martín, M. E.; Aguilar, M. A. Theoretical Study of the Dual Fluorescence of 4-(N,N-Dimethylamino)benzonitrile in Solution. *Journal of Chemical Theory and Computation* **2010**, *6*, 2445–2454, PMID: 26613498.

## **Supporting Information**

## Supporting information: active spaces, excitation energies and reference data

### NEVPT2

#### Active space size

	ASF(S)	I-ASF(S)	ASF(T)	I-ASF(T)	ASF(QRO)	I-ASF(QRO)
acetamide	(8, 7)	(8, 7)	(4, 4)	(4, 4)	(4, 4)	(4, 4)
adenine	(8, 8)	(10, 9)	(8, 8)	(8, 8)	(10, 9)	(12, 10)
benzoquinone						
ne	(16, 12)	(16, 12)	(8, 8)	(8, 8)	(8, 8)	(14, 11)
cyclopenta						
diene	(4, 4)	(8, 8)	(4, 4)	(4, 4)	(4, 4)	(8, 8)
cyclopropane						
ne	(4, 4)	(10, 10)	(6, 5)	(6, 5)	(4, 4)	(4, 4)
cytosine	(6, 6)	(8, 7)	(8, 7)	(8, 7)	(6, 6)	(10, 8)
formamide	(8, 7)	(8, 7)	(6, 6)	(6, 6)	(4, 4)	(4, 4)
hexatriene	(6, 6)	(6, 6)	(6, 6)	(6, 6)	(6, 6)	(6, 6)
norbornadiene						
ene	(6, 5)	(6, 5)	(4, 4)	(4, 4)	(6, 5)	(6, 5)
octatetraene						
e	(8, 8)	(8, 8)	(8, 8)	(8, 8)	(8, 8)	(8, 8)
propanamide						
de	(8, 5)	(8, 5)	(4, 4)	(4, 4)	(4, 4)	(4, 4)
pyrrole	(6, 5)	(6, 5)	(6, 5)	(6, 5)	(6, 5)	(6, 5)
thymine	(8, 7)	(10, 8)	(8, 7)	(8, 7)	(8, 7)	(8, 7)
triazine	(6, 6)	(10, 10)	(10, 8)	(10, 8)	(10, 8)	(10, 8)
uracil	(10, 8)	(12, 10)	(18, 12)	(18, 12)	(8, 7)	(8, 7)
acetaldehyde						
de	(8, 6)	(8, 7)	(4, 3)	(8, 8)	(4, 3)	(10, 9)
acetone	(8, 7)	(8, 7)	(4, 3)	(10, 9)	(4, 3)	(4, 3)
benzene	(6, 6)	(6, 6)	(6, 6)	(6, 6)	(6, 6)	(6, 6)
butadiene	(4, 4)	(4, 4)	(4, 4)	(6, 6)	(4, 4)	(4, 4)
DMABN	(12, 12)	(12, 12)	(12, 12)	(14, 13)	(14, 13)	(14, 13)
ethylene	(4, 3)	(6, 5)	(4, 3)	(8, 8)	(4, 3)	(4, 3)
formaldehyde						
de	(8, 7)	(8, 7)	(4, 3)	(8, 7)	(4, 3)	(6, 5)
furan	(8, 7)	(8, 7)	(4, 4)	(4, 4)	(6, 5)	(6, 5)
hexatriene	(6, 6)	(6, 6)	(6, 6)	(6, 6)	(6, 6)	(6, 6)
naphthalene						
e	(10, 10)	(10, 10)	(10, 10)	(10, 10)	(10, 10)	(10, 10)
pNA	(8, 8)	(12, 11)	(8, 8)	(12, 11)	(8, 8)	(14, 12)
pyrazine	(6, 6)	(8, 8)	(10, 8)	(10, 8)	(10, 8)	(10, 8)
pyridazine	(6, 5)	(14, 11)	(10, 8)	(10, 9)	(10, 8)	(10, 8)
pyridine	(6, 6)	(6, 6)	(6, 6)	(6, 6)	(6, 6)	(6, 6)
pyrimidine	(12, 9)	(14, 11)	(10, 9)	(10, 9)	(8, 7)	(6, 6)
stetrazine	(10, 8)	(18, 15)	(10, 8)	(16, 15)	(12, 9)	(16, 14)
water	(6, 6)	(6, 6)	(4, 5)	(4, 5)	(4, 5)	(4, 5)

## NEVPT2

## Excitation energy

	ASF(S)	I-ASF(S)	ASF(T)	I-ASF(T)	ASF(QRO)	I-ASF(QRO)
acetamide	5.64343345	5.64330467	7.09280837	7.09280837	7.09275634	7.09273819
adenine	5.65613128	5.5889308	5.65624156	5.65624156	5.58898461	5.48635054
benzoquinone						
cyclopentadiene	4.36836036	4.36830639	4.33419831	4.33419831	4.33417706	4.36119318
cyclopropane	6.77158965	5.54055804	6.77146649	6.77146649	6.77148616	6.72892849
cystosine	6.77423432	6.85655922		0	6.77422649	6.77412997
formamide	4.81346222	4.72733609	4.72734706	4.72734706	4.81328299	4.75817179
hexatriene	5.5499178	5.54991731	7.18006095	7.18006095	7.30203618	7.30203617
norbornadiene	5.58893002	5.58889384	5.58890202	5.58890202	5.58888908	5.58890346
octatetraene		5.16117957	5.20600538	5.20600538		5.16623861
propanamide	4.73519275	4.73519182	4.73519463	4.73519463	4.73518958	4.73519366
pyrrole	6.59308169	6.59310072	6.59310243	6.59310243	6.59313402	6.59313453
thymine	5.21685939	5.15543352	5.2168842	5.2168842	5.21691264	5.21693238
triazine	6.03980451	5.90794876	4.91331475	4.91331475	4.9132483	4.91326429
uracil	5.29283054	5.36507066			5.37743657	5.37742944
acetaldehyde						
acetone	4.31900153	4.30609937	4.47071467	4.41232421	4.47071006	4.4267007
benzene	4.47929092	4.47929213	4.6164652	4.53809473	4.6164366	4.61647788
butadiene	5.22424248	5.22480494	5.22487716	5.2241681	5.22460946	5.22475642
DMABN	6.80949154	6.80949038	6.80955244	6.83140441	6.80956129	6.80956068
ethylene	8.01458156	8.03493114	8.00414935	8.08769267	8.0044892	8.00450239
formaldehyde						
furan	3.95491066	3.95490704	4.15333256	3.95490909	4.15334615	3.97657275
hexatriene	6.7812056	6.78120808	6.83143236	6.83143236	6.76845178	6.76845178
naphthalene	5.59375104	5.5937216	5.59372902	5.59373827	5.59372462	5.59369869
pNA	4.42716715	4.42693123	4.4269286	4.42692749	4.42693897	4.42693902
pyrazine	5.05740307	5.07146102	5.05740153	5.07140728	5.0573919	5.06908231
pyridazine	5.28256734	5.22131375	4.21421431	4.21422204	4.21423722	4.21420643
pyridine	5.85469816		3.83124125	4.32885957	3.83118508	3.83121273
pyrimidine	5.3952249	5.39522658	5.39528588	5.39528665	5.39518559	5.39518506
stetrazine	5.65162169	5.58535052	5.08914791	5.08899139	5.11252487	5.06943752
water	2.67861156		2.3364637	3.28391198	2.42235772	2.65987127
	9.47067101	9.47066676	7.60250067	7.60250097	7.6025048	7.60249942

## Reference Excitation values

acetamide	5.8
adenine	5.2
benzoquino	
ne	2.8
cyclopenta	
diene	5.51
cycloprope	
ne	6.76
cytosine	4.68
formamide	5.63
hexatriene	5.31
norbornadi	
ene	5.34
octatetraen	
e	4.64
propanami	
de	5.72
pyrrole	6.31
thymine	4.94
triazine	6.31
uracil	4.9
acetaldehy	
de	4.27
acetone	4.44
benzene	4.99
butadiene	6.38
DMABN	4.87
ethylene	8.16
formaldehy	
de	3.92
furan	6.32
hexatriene	5.32
naphthalen	
e	4.24
pNA	4.62
pyrazine	4.04
pyridazine	3.67
pyridine	5.06
pyrimidine	4.38
stetrazine	2.56
water	7.61